The Pennsylvania State University

The Graduate School

CONTROLLING SELECTIVITY OF PLATINUM DEPOSITION ON PARTIALLY EXCHANGED $Cu_{2-x}S$-CdS NANOPARTICLES

A Thesis in

Chemistry

by

Jonathan Ackerman

Submitted in Partial Fulfillment
of the Requirements
for the Degree of

Master of Science

December 2019

The thesis of Jonathan Ackerman was reviewed and approved* by the following:

Raymond E. Schaak
DuPont Professor of Materials Chemistry
Thesis Advisor

Ben J. Lear
Associate Professor of Chemistry

John B. Asbury
Professor of Chemistry

Philip C. Bevilacqua
Distinguished Professor of Chemistry and Biochemistry and Molecular Biology
Head of the Department or Chair of the Graduate Program

*Signatures are on file in the Graduate School

ABSTRACT

As the applications of nanotechnology become more advanced, the need for the ability to synthesize more complex nanomaterials. Nanoparticles, in particular, have found application in sensing[1-3], catalysis[4-8], biomedicine[3,9] and other fields utilizing increasingly complex systems. Already there are systems that have been proposed that cannot be made through existing syntheses, such as a z-scheme trimer nanoparticle similar to the powder-based system developed by Maeda et. al.[4] In order to enable the continued development of both the applications and our understanding of these systems, we first need to advance our ability to synthesize novel, complex nanoparticle systems. Developing novel hybrid nanoparticles, in which multiple solid domains are connected through a solid-solid interface, is one route that is of particular interest. These particles allow for cooperative effects that are not possible through organic linkages, such as the enhancement of the catalytic activity of Au and Pt nanoparticles via the addition of Fe_3O_4 observed by Sun et. al.[5] However, developing hybrid systems with three or more solid material domains requires the ability to control the arrangement of the domains to achieve the desired configuration. While strategies analogous to the protection/deprotection techniques used in organic synthesis have been developed[10-12], a deeper understanding of factors governing the selectivity of a deposited material for a particular domain in a hybrid nanoparticle is essential for the development of more generalized and higher yield synthetic protocols. In this work, we explore the factors that lead to the selective deposition of Pt on $Cu_{2-x}S$-CdS nanorod and the factors that led the selectivity inversion observed by Fenton et. al. in the deposition onto $Cu_{2-x}S$-CdS nanoparticles[13].

TABLE OF CONTENTS

LIST OF FIGURES

ACKNOWLEDGEMENTS

There are too many people that have helped me over the past few years to list all of them here, but there are a few people who I feel need to be mentioned here.

First, Yifan Sun and Robert Lord for helping keep me sane when I was overwhelmed. Late nights on the Talos would have been much worse if they had not been willing to take my calls and even come in to help me troubleshoot problems.

Cameron Holder, Joseph Dawson, and Caleb Uitvlugt for reminding me that there is life outside of the lab. Having a hobby to take a break from science every now and then made even bad weeks a lot more bearable.

Dr. Raymond Schaak, for far too many things. He has been amazingly patient and insightful with his advice and I know for a fact that I could not have made it this far without him. His efforts to help me become a better researcher appreciated more than I can put into words.

Finally, my parent who have supported me through everything and helped me see the forest through the trees when I was overly stressed about something.

And, of course, I would like to thank the Schaak lab for all fun moments throughout the years and the help, both scientific and personal, that they have given me.

This work was supported by the U.S. National Science Foundation via Grant CHE-1410061 and Grant CHE-1707830. TEM imaging was performed in the Penn State Microscopy and Cytometry facility. HRTEM imaging, S/TEM imaging, and EDS mapping were performed at the Materials Characterization Lab of the Penn State Materials Research Institute.

Chapter 1

SELECTIVITY OF Pt DEPOSITION ON Cu2-xS-CdS NANORODS

Introduction

Multicomponent nanoparticles combine several nanoscale material domains into a single particle in order to achieve effects beyond any single material system. Single component nanoparticles linked through complex organic ligands, like DNA, or assembled into larger systems are examples of multicomponent particles that have found use in sensing[2] and drug delivery[9] applications. Particles with a solid-state interface between material components, as opposed to organic linkers, additionally allow for synergistic effects that these other classes do not. These particles, referred to herein as hybrid nanoparticles, can incorporate materials with different properties that can interact with each other and even modify the properties of the other material. As an example, Sun and coworkers demonstrated the enhanced catalytic activity of Au-Fe_3O_4 and Pt-Fe_3O_4 for the CO oxidation reaction as compared to the single component Au and Pt nanoparticles[5]. Hybrid particles have been used to add a desired property, like magnetic or optical response, to enable the magnetic separation and recovery of particles as demonstrated by Williams and coworkers[14] or to produce an additional axis of sensing as can be seen in work from the Sun group[3]. Additionally, by creating an interface between metal and semiconductor domains, the resultant charge separation can be used for catalytic applications[15], such as CdSe seeded CdS rods with a Pt domain as shown by Alivisatos[7,8], Lian[4] and others.

Hybrid nanoparticles are nanoscale particles comprised of two or more hard material cores connected through solid-solid interfaces and stabilized by surfactant, or ligand, molecules that provide colloidal dispersibility in, typically non-polar, solvents.

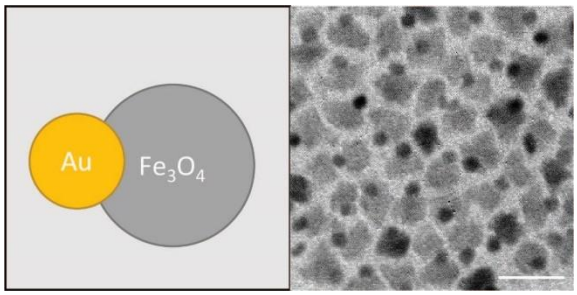

Figure 1: Schematic representation and TEM of Au-Fe_3O_4 nanoparticles

In the simplest case, hybrid nanoparticles are formed through the reduction of a metal salt in the presence of both a surfactant molecule, which binds to the surface and prevents agglomeration of the particles, and a premade "seed" particle on to which the new material will nucleate and grow. The most common of these systems are comprised of two spherical particles, but other morphologies do exist, including rods[4,7,8,15], plates[16], and tetrapods[17]. The synthesis of a hybrid nanoparticle takes advantage of the energy barrier that must be overcome during the nucleation stage of a typical single component nanoparticle. In this homonucleation process, small, unstable clusters of atoms that are formed must reach a minimum "critical radius" before they are stable and can undergo growth[18]. If, however, a pre-existing surface is present in the reaction on which the material can nucleate, the energy barrier for nucleation will be decreased. Thus, by selecting conditions that prevent a significant portion of the material from forming unsupported nuclei, heteronucleation and growth can be favored, leading to a hybrid particle. This process, of course, requires a preformed seed particle that is stable under the reaction conditions. Other mechanisms for growth of new domains do exist, such as solid-liquid-solid growth[19], in which a material becomes supersaturated with another and a solid interface is formed as the two segregate, and alloying-dealloying[20,21] methods, in which one component of an alloy particle is extracted chemically, but these are more limited in terms of suitable materials and still require a seed particle. These mechanisms are important for reactions in which a new material is grown between existing hybrid domains, based on the formation of more favorable interfaces than the

material/ligand and solution[22] while seeded growth is unable to access the interface between to existing domains.

As with single component nanoparticles, the dispersibility, as well as biocompatibility[3,23], of these particles can be tuned through the ligand functionalization. These ligands bind to the surface of the hard material domains through functional groups, such as amines[24] and thiols[25]. The tails of these molecules orient out from the surface and toward the solvent. The length and structure of these tail groups will dictate a number of properties, including electronic properties[26] and the morphology[27] of the particle and can be used in sensing applications[1], of bacteria in contaminated water for example, or to control the catalytic activity of the core material[28]. In the same way, the identity of the functional group through which the ligand binds will determine how strongly the ligand is bound to the surface nanoparticle. This can be used to replace ligands[29,30] used in the synthesis of the nanoparticle with ones that bind more strongly and impart the desired properties. In the case of hybrid particles each domain has the potential for different ligation[3], which can be a route to tuning the properties of each surface individually, for example the Sun group used a Au-Fe_3O_4 hybrid particle in which they claimed each domain was functionalized with a separate ligand that could each be used for sensing applications to produce a dual functional probe capable of magnetic and optical responses to indicate two different analytes. However, the complexity of these systems grows rapidly as the number of domains increases and the characterization requires nanoscale resolution to determine which domain each ligand is bound to. This makes research into these systems challenging and most hybrid systems do not attempt to create separate ligand environments for the individual domains.

The formation and reactivity of hybrid particles can be thought of in a similar manner to small molecules. Addition, elimination, insertion, and coupling reactions can modify hybrid nanoparticles and expand their complexity. For example, Buck et. al. demonstrated three sequential seeded growth reactions to produce a four-component tetramer nanoparticle comprised

of Cu_9S_5-Au-Pt-Fe_3O_4[31]. Hodges et. al. demonstrated the use of ZnO as a protecting group for Au-Fe_3O_4 in which the ZnO removed through etching with oleic acid[11]. This system was designed as an analog to the protection/deprotection techniques used in organic synthesis, where the ZnO can be used to protect the preferred domain and direct subsequent nucleation to a less favorable domain. Similarly, Chen and coworkers demonstrated a protection-deprotection scheme using SiO_2 though this required the use of a polymeric ligand to produce the asymmetric SiO_2 mask[12]. Read et. al. demonstrated a method of inserting a Ge domain between a preexisting Au-Fe_3O_4 interface through a solution-liquid-solid[19] reaction in which a supersaturated Au-Ge alloy is formed from which a Ge domain crystalized. Since this solution-liquid-solid mechanism does not rely on surface nucleation to form a new domain, it can be used to access interfaces, like the Au-Fe_3O_4, that seeded growth cannot. Lastly, the Manna group demonstrated a method of linking multiple Au-CdS hybrid particles together through Au domains[32] using iodine to replace the ligands on the surface of the Au domains and inducing a controlled agglomeration. This "nanowelding" or coupling of particles enables a route to the synthesis of higher order hybrid nanoparticles than addition alone, but still requires at least a two-component particle to create anything more than large agglomerations of Au.

However, unlike the broad applications of organic reactions to the synthesis of complex molecules, the library of possible hybrid nanoparticle systems is limited to a smaller collection of specific examples for many of these reaction types. Addition of a new material domain is the most well understood and explored, with known conditions for the growth of a wide range of material classes[3,5,21,22,32-34]. However, the "seed" material onto which the new material is grown is limited to a small number of systems as a majority of these seeded growth methods require a noble metal particle, usually gold or platinum. This limitation is particularly problematic in that it limits the types of interfaces that can be synthesized, which in turn limits the application of hybrid nanoparticles. As an example, z-scheme trimers capable of splitting water in a single step

requires both a catalyst capable of the oxidation of water to oxygen and one capable of the reduction of protons to hydrogen each connected through a solid stat interface to a light absorbing material with an appropriate band gap and band edge alignment[35]. One example requiring nanoparticles of Mn_3O_4 and core-shell Rh/Cr_2O_3 cocatalysts on a powder consisting of a solid solution of GaN and ZnO relies on the formation of oxide-oxide interfaces. These interfaces are difficult to achieve through seeded growth methods due to the tendency of the oxides to homonucleate rather than nucleate on the surface the seed, though an Fe_3O_4-MnO particle has been synthesized by Lee et. al.[34]

These addition reactions can be performed using other hybrid particles as seeds, for example, Buck et. al.[31] showed the sequential addition of three materials, Au, Fe_3O_4, and Cu_9S_5, to a Pt seed to produce a four component hybrid nanoparticle. Due to the increasing number of sequential reactions, however, morphological yield becomes an issue with higher order systems which limits the scope of systems that are synthetically accessible despite a larger number that would be expected to be possible. In an ideal hybrid particle with only two spherical domains, the placement of the second domain can always be related to any other placement through rotation. For example, as shown in Figure 2, growth on different positions on a spherical particle can be related through a rotation of the particle.

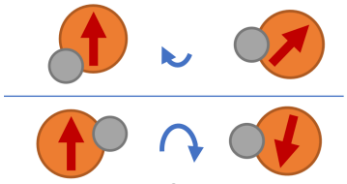

Figure 1: Schematic demonstrating orientational indistinguishability of two component hybrid nanoparticles.

However, this is not the case in higher order systems or systems with non-spherical domains. In these systems, the location of the new domain can become important for the properties of the overall system. It has been shown, for example, that the placement of a spherical catalytic domain on a rod-like light absorbing domain can affect the efficiency of the system. Specifically, Alivisatos and coworkers showed that longer CdS rods with more distance between the CdSe core and the Pt domain, which used the electrons to reduce H^+ to H_2, would improve the

activity of the system by increasing the amount of charge separation[7]. Unfortunately, controlling the location of a domain through seeded growth remains challenging as it will often be dictated by the characteristics of the seed particle without significant tunablity and it can even be difficult to predict which domain in a higher order seed particle the deposition will ultimately favor. Factors such as lattice matching, bond strengths at the interface, and even electronic effects can affect the selectivity of a material for one domain over another and this selectivity can exist even in systems in which both seed domains can individually support the nucleation of the new material. Bradley et. al. showed that three sulfides, CdS, PbS, and Cu_xS_y, would preferentially grow on the Au domain of a Pt-Au hybrid particles, even though the sulfide would grow on either Pt or Au single component seeds[36]. This was rationalized though the strong Au-S bonding that would be present in these trimers. A similar study on the growth of Ag on Pt-F_3O_4 hybrids showed that the growth process is not always as straight forward. Hodges et. al. showed that the Ag would first deposit indiscriminately and then migrate to the Pt domain through surface diffusion.[37] Banin and coworkers observed that Au was localized to the CdSe portion of the CdSe seeded CdS rods.[38] The authors explained this selectivity through an electronic effect which led to the preferential reduction of Au at the location of the CdSe seed. Addressing the need for more controllable morphological features and interface design requires a deeper understanding of the factors that control material deposition in multicomponent nanoparticles and a method for exploiting these factors.

Partial Cation Exchange

One method of expanding the library of materials available to nanoparticle synthesis is the post-synthetic modification of preexisting domains. Rather than simply growing the specific target material domain, this approach would allow a synthetically accessible system to be

converted into the desired hybrid system. For example, Fenton et. al. demonstrated the conversion of the MnO domain of a Pt-MnO nanoparticle into several different materials including Ag_2Se.[39] For chalcogenides, particularly sulfides and selenides, cation exchange can enable the conversion of one material to another related material by replacing the host cations with the desired ones. In an early example of this, the Alivisatos group showed the conversion of CdSe to Ag_2Se through the replacement of the Cd^{2+} cations with Ag^{+} with methanol and then the conversion back to CdSe with the addition of Cd^{2+} and tributylphosphine.[40] While the guest and host cations are exchanging, the anion sublattice has been shown to be maintained often resulting in the exchange forming a structurally similar phase to that of the initial material.[41,42]

In order to extract the host cations and add the desired cations, an appropriate Lewis base must be used to help drive the reaction. This base must be chosen for its stronger interaction with the host ion than the guest, which is determined by the relative hardnesses[43] of the ions and the base. The absolute hardness as defined by Pearson and Parr is the derivative of the chemical potential[44] with respect to the number of electrons and can be viewed in terms of the disproportionation reaction,

$$S + S \rightarrow S^{+} + S^{-}$$

where small changes in energy are classified as soft and large changes as hard. In the case of bases, softness broadly corresponds to higher polarizability and lower electronegativity, and is associated with easily oxidized atoms. With cations, hardness increases as charge increases and size decreases, with outer electrons that can be easily excited. By selecting a base with a hardness that better matches the hardness of the host cation, the exchange will be driven thermodynamically by the formation of the preferred acid-base pair.

The process of exchange occurs through a process mediated by diffusion, though the diffusion pathways may not be the same for all material systems. Work by Groeneveld et. al.[45] suggests a mechanism by which the guest ion is able to replace a surface host ion and then slowly

diffuse through the anion lattice via Frenkel defects caused by host dislocations. In a similar but distinct manner, work on other systems by Wang and coworkers[46] has demonstrated that charged vacancies are energetically preferable and better match the observed exchange rate. In this process, a host ion first leaves the crystal and creates a vacancy that can propagate through a structure, allowing ionic conduction. This difference in mechanism may be explained by miscibility, where miscible materials exchange through a Frenkel defect, in which a cation leaves its position in the lattice and takes up an interstitial position leaving behind a vacancy.

By arresting the cation exchange reaction before completion, a partially exchanged system can be produced, with domains of both host material and the exchanged material in the same particle. In nanoparticle systems, this can be used to generate new interfaces within the template of the initial particle, essentially creating a hybrid particle. The orientation of the interface will be dictated by the crystal structure of the two materials as well as the reaction conditions.[47] The chalcogenide-chalcogenide interfaces formed through partial cation exchange are particularly challenging to form via seeded growth techniques. This alone makes partial cation exchange an excellent complement to seeded growth. However, the ability to use cation exchange to alter the hybrid particle in a controllable way after the seeded growth reaction that truly open new avenues in hybrid synthesis. Unlike seeded growth methods, the morphology of partially exchanged particles can be designed separately from the material choices and the segmentation of materials can be altered after the reaction through further cation exchange reactions. Fenton et. al. demonstrated that one domain of a Pt-MnO hybrid nanoparticle could undergo a series of cation and even anion exchange reactions without destroying the interface between the two domains.[39] Thus, a partially exchanged particle could be used as a template to direct the deposition of a new material through seeded growth and then undergo a subsequent exchange to a final, desired material. This means that partially exchanged particles can serve as ideal templates to direct seeded growth reactions without the same design limitations as purely seeded growth schemes.

This Investigation

Incorporating seeded growth and partial cation exchange techniques enables novel hybrid systems with interfaces that cannot be produced with either individually. The use of partial exchange to direct the growth of the material deposited via seeded growth is a powerful design tool that can enable otherwise difficult morphological control, such as deposition on a central ring of a tunable size, as depicted in Figure 3 rather than simply the tips of a nanorod[48] or the sides of as nanoplate[16]. However, before these and other systems can be accessed, the parameters that control the selectivity of the deposited material for the desired chalcogenide domain need to be determined. In seeded growth reactions, the new material favors one material, typically a noble metal, over the other under most conditions. This selectivity for a certain material over another has been rationalized via the epitaxial lattice matching of the two materials[5], though this does not always hold true[31]. Selectivity can be forced by the inability of a reaction with one domain, due to passivation of the surface of one domain as demonstrated by Hodges et. al.,[10] however, the protecting domain is not always easy to remove and the additional steps required would drastically reduce the yield of the final product. The ability to design a template through cation exchange that promotes the desired deposition pattern and then post-synthetically alter that chalcogenide domain decouples the material selectivity from the final morphology.[13]

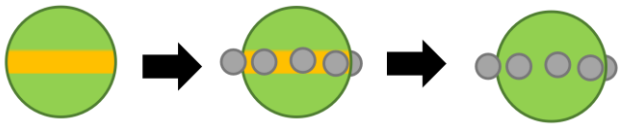

Figure 2: Schematic illustration of ring like deposition on a partially exchanged spherical particle

In order to investigate the factors involved in determining both the nature and degree of selectivity with respect to two sulfide materials in a partially exchanged nanoparticle, we investigated the deposition of platinum through established seeded growth techniques onto a roxbyite $Cu_{2-x}S$ rod partially exchanged with cadmium to form a two domain $Cu_{2-x}S$ nanorod

template. Roxbyite copper sulfide was chosen as the host material for the exchange reaction due to the copper vacancies present in the crystal structure[49], which enabled milder conditions and a more efficient reaction in regards to the amount of guest cations required. The choice to exchange with cadmium was due to the consistency of exchange pattern achieved using known procedures, though work on these reactions is ongoing. Finally, platinum was chosen as the deposition material due to the existence of seeded growth procedures for platinum on copper sulfide[50] and the lack of exchange with either domain of the nanoparticle. In contrast, gold was not selected due to its potential to exchange with copper sulfide to form gold sulfide.[51]

In order to explore the effects of the morphology on the deposition selectivity, copper-sulfide nanorods were used for the exchange with cadmium. The results of the platinum deposition reaction could then be compared to the results reported by Fenton et. al.[13] in which platinum deposited selectively on the $Cu_{2-x}S$ domain of a $Cu_{2-x}S$-CdS partially exchanged spherical nanoparticle. These particles consist of the same materials and are made through similar reactions, but with a spherical morphology rather than a rod-like one, making these systems the best choice for isolating and investigating the effects of morphology, and any resultant surface chemistry differences, on the seeded growth of Pt.

Additionally, the anisotropy of the rods enables easier characterization of the particles, since there is less chance of the two domains overlapping in TEM images and EDS maps. Using only TEM based techniques there is no way to differentiate between overlapping but spatially discreet domains and colocalization via alloying for example, barring tomography. This exploration of morphological differences is important in order to move beyond spherical template particles which do not offer the same level of unique deposition complexity as anisotropic particles, like nanorods. In the simplest case, as

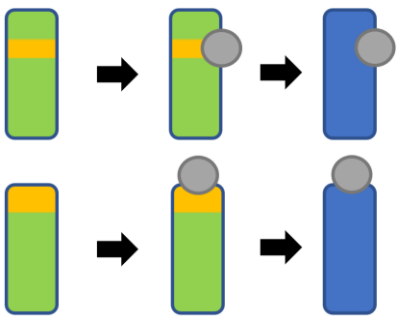

Figure 3: Schematic illustration of templated deposition onto a partially exchanged nanorod

shown in Figure 3, deposition of a single domain onto a spherical seed particle results in a "dumbbell" particle which can be related through rotation to another "dumbbell" particle of the same composition. Rods, on the other hand, have symmetrically distinct tips and sides, which means that directing deposition to a location on the side of a partially exchanged nanorod and then subsequently exchanging that rod to a single material does not nullify the uniqueness of that location.

In order to determine which factors control which material a newly deposited domains will nucleate on and how to tune the extent of this selectivity, we undertook an investigation aimed at exploring several factors, including morphology, rate of reduction and surface, and reaction time. By understanding how these factors affect the deposition on partially exchanged particles we hope to enable greater the control over the deposition process and the synthesis of rationally designed hybrid particles through the use of partially exchanged, segmented nanoparticles as templated seeds. We anticipate that these systems will provide the easiest route to the synthesis of hybrid particles with chalcogenide-chalcogenide interfaces thereby expanding the library of synthetically accessible hybrid systems. Additionally, we expect that these systems will offer a method of targeted deposition onto chalcogenide nanoparticles based on the design of an initial partially exchanged nanoparticle and eventual exchange to the desired material.

Our initial expectations were that morphology would be mostly irrelevant and the selectivity would be dictated by the kinetics of the reaction. We did not anticipate that the material selectivity would change from copper sulfide, as reported on the spheres,[13] to cadmium sulfide, since the materials remained the same, however, we did expect that the degree of selectivity might decrease, with the difference between the deposition on each material becoming more similar, as the rate of reduction increased. As such, we planned to vary the concentrations of the platinum precursor, platinum (II) acetylacetonate, and the reducing agent, oleylamine, as well

as the time and temperature of the reaction, starting with the conditions reported for the deposition onto the partially exchanged spheres.

Experimental

Materials

Octadecene [ODE, 90%, technical grade], technical grade oleylamine [tg-OLAM, 70%], di-tert-butyl disulfide [97%], trioctylphosphine oxide [TOPO, ≥90%], tert-dodecanethiol [t-DDT, mixture of isomers 98.5%], 1-dodecanethiol [DDT, ≥98%], Copper(II) acetylacetonate [$Cu(acac)_2$ 97%], copper(II) chloride [$CuCl_2$, 97%], copper(II) nitrate trihydrate [$Cu(NO_3)_2 \cdot 3H_2O$], Dioctyl ether (DOE, 99%), and platinum(II) acetylacetonate [Pt(acac)2, 97%] were purchased from Sigma Aldrich. Trioctylphosphine [TOP, >85%] was purchased from TCI America. Benzyl ether [99%] was purchased from Acros Organics. Cadmium(II) acetate dihydrate [Cd(OAc)2·2H2O, 99.999% trace metals basis] was purchased from Alfa Aesar. All solvents, including hexanes, isopropanol [IPA], toluene, and acetone, were of analytical grade. tg-OLAM was distilled using standard vacuum distillation techniques to produce high-purity oleylamine [hp-OLAM].

Methods

Synthesis of $Cu_{2-x}S$ rods

Rod-shaped $Cu_{2-x}S$ nanoparticles were synthesized using a modification of a published procedure[13]. $Cu(NO_3)_2 \cdot 3H_2O$ (281 mg), TOPO (2.9 g), TOP (320 uL) and ODE (15 mL) were combined in a 100 mL 3-neck flask equipped with a reflux condenser, gas flow adapter, thermocouple, rubber septum, and magnetic stir bar. This mixture was placed under vacuum, heated

to 80°C, and held at this temperature for 30 minutes. The flask was placed under a blanket of Ar after cycling with vacuum and Ar three times. The reaction temperature was increased to 180°C within 5 minutes by placing the flask in a pre-heated heating mantle. As the temperature was increasing, 7.5 mL of a 10:1 mixture of t-DDT:DDT was rapidly injected, resulting in a yellow-colored solution. The flask was held at 180°C for 5 minutes before being cooled rapidly by removing the heating. Upon reaching ~40°C, 2 mL of toluene was added to the reaction mixture. The resulting product was precipitated by addition of IPA, followed by centrifugation and resuspension in hexanes. The centrifugation / resuspension process was repeated twice more, and the final brown product was resuspended in 6 mL of hexanes (~6 mg/mL) for characterization and use in further reactions.

Synthesis of $Cu_{2-x}S$ spheres

Spherical $Cu_{2-x}S$ nanoparticles were synthesized using a modification of a published procedure[13]. $CuCl_2$ (341 mg), hp-OLAM (47.2 mL), and ODE (11.8 mL) were combined in a 100 mL 3-neck round-bottom flask equipped as described above. This mixture was placed under vacuum, heated to 100°C, and held at this temperature for 30 minutes. The flask was placed under an Ar flow after cycling with Ar and vacuum three times, then heated to 200 °C for 60 minutes, degassing at this temperature under Ar flow to remove gaseous side products formed during the dissolution of $CuCl_2$ in OLAM. The solution was cooled to 180°C and 8 mL of di-tert-butyl disulfide (under Ar) was rapidly injected, turning the clear yellow solution to turbid brown. Once the temperature restabilized at 180°C, the reaction was allowed to proceed for 40 minutes. The product was isolated by addition of IPA into the reaction mixture followed by centrifugation and resuspension in toluene. The centrifugation / resuspension process was repeated twice more, adding a few additional drops of OLAM in the third washing step, and the final black/brown product was resuspended in 10 mL of hexanes (~6 mg/mL) for characterization and use in further reactions.

Synthesis of smaller $Cu_{1.94}S$ spheres

Spherical $Cu_{1.94}S$ nanoparticles were synthesized using a modification of a published procedure.[52] $Cu(acac)_2$ (500 mg), DDT (20 mL), and DOE (5 mL) were degassed for one hour then heated to 215˚C under argon for one hour. After cooling the reaction mixture to room temperature, the product was precipitated by the addition of IPA and collected by centrifugation. After resuspension in hexanes, the product was washed twice with IPA. The product was resuspended in 5 mL of hexanes for characterization and further use.

Cation exchange reactions with Cd^{2+}

Partial cation exchange reactions with Cd^{2+} were performed through adaptation of a published procedure[13]. A Cd^{2+} solution was prepared by combining $Cd(OAc)_2 \cdot 2H_2O$ (245 mg), hp-OLAM (8 mL), ODE (2 mL), and benzyl ether (15 mL) in a 50 mL 3-neck flask equipped as described above. This mixture was placed under vacuum and heated to 100°C for 60 minutes, placed under a blanket of Ar, then cooled to 50°C. During this time, 12 mg of copper sulfide nanorods were resuspended in 3 mL of TOP and sonicated for 45 minutes. The nanoparticle/TOP suspension was rapidly injected into the reaction flask and allowed to react for 60 minutes. The reaction was quenched after this time by injection of 8 mL of ice-cold acetone into the flask, which was then placed into an ice bath. The product was precipitated by the addition of IPA and collected by centrifugation. After resuspension in hexanes, the product was washed twice with IPA. The product was resuspended in 5 mL of hexanes for characterization and further use.

Standard synthesis of Pt-$Cu_{2-x}S$-CdS rods

Pt was grown on pre-formed $Cu_{2-x}S$–CdS nanorods through an adaptation of a published procedure for growing Pt on metal sulfides[13]. The growth solution was prepared by combining 5 mg of $Pt(acac)_2$, 7 mL of ODE, and 50 μL of tg-OLAM in a 50 mL 3-neck flask equipped as described above. Approx. 0.75 mg of CdS– $Cu_{2-x}S$ nanorods were suspended in 0.5 mL of ODE,

which was added directly to the reaction flask. The flask was placed under vacuum and held at 50°C for 30 minutes, then was cycled with Ar and vacuum three times and placed under Ar. The reaction temperature was increased to 130°C for 2.5 hours, then cooled to room temperature. The black suspension was centrifuged without any IPA/acetone and the black-colored supernatant was discarded. The product was resuspended in toluene, precipitated with IPA, and centrifuged. The centrifugation/redispersion process was repeated once more. The final product was dispersed in hexanes for further use and characterization.

Using increased concentrations synthesis of $Cu_{2-x}S$-CdS-Pt rods and $Cu_{2-x}S$-PtCdS-Pt spheres

A modification to the previously described synthesis of $Cu_{2-x}S$-CdS-Pt rods was also used. In this reaction the growth solution was prepared by combining 20 mg of $Pt(acac)_2$, 7 mL of ODE, and 200 μL of tg-OLAM in a 50 mL 3-neck flask equipped as described above. Approx. 3 mg of CdS– $Cu_{2-x}S$ nanorods or 1.5 mg each of $Cu_{2-x}S$ and CdS nanoparticles were suspended in 0.5 mL of ODE, which was added directly to the reaction flask. All other conditions are identical to the standard synthesis. Variations of this procedure were used throughout this investigation and are described below.

Aliquot study of synthesis of $Cu_{1.94}S$-Pt and CdS-Pt spheres and $Cu_{2-x}S$-CdS-Pt rods

Using conditions previously described in the increased concentration procedure, aliquots were taken from the synthesis of the $Cu_{2-x}S$-CdS-Pt rods and the $Cu_{1.94}S$-Pt and CdS-Pt spheres. Aliquots were from the synthesis of $Cu_{2-x}S$-CdS-Pt rods at 15, 30, 60, 90, 120, and 150 minutes and at 5 and 120 minutes were from the synthesis of $Cu_{1.94}S$-Pt and CdS-Pt spheres. All other conditions are identical to the increased concentration synthesis.

OLAM experiments in synthesis of $Cu_{1.94}S$-Pt and CdS-Pt spheres and $Cu_{1.94}S$-CdS-Pt rods

Using conditions previously described in the increased concentration procedure, the concentration of OLAM was varied in the synthesis of the $Cu_{2-x}S$-CdS-Pt rods and the $Cu_{1.94}S$-Pt and CdS-Pt spheres. In the synthesis of the $Cu_{2-x}S$-CdS-Pt rods, the 200 μL of OLAM was

replaced with 50 μL, 100 μL, or 150 μL. In the synthesis of the $Cu_{1.94}S$-Pt and CdS-Pt spheres, the 200 μL of OLAM was replaced with 25 μL, 100 μL. All other conditions are identical to the increased concentration synthesis.

$Pt(acac)_2$ experiments in synthesis of $Cu_{2-x}S$-CdS-Pt rods

Using conditions previously described in the increased concentration procedure, the 20 mg amount of $Pt(acac)_2$ in the synthesis of the $Cu_{2-x}S$-CdS-Pt rods was replaced with 10 mg and 15 mg. All other conditions are identical to the increased concentration synthesis.

Temperature experiments in synthesis of $Cu_{1.94}S$-Pt and CdS-Pt spheres

Using conditions previously described in the increased concentration procedure, the 130^{o} C temperature was changed to in the synthesis of the $Cu_{1.94}S$-Pt and CdS-Pt spheres to 100 ^{o} C, 140 ^{o} C, and 160^{o} C. All other conditions are identical to the increased concentration synthesis.

Characterization

Transmission electron microscopy (TEM) images were collected from a JEOL 1200 EX II microscope operating at 80 kV. High angle annular dark field scanning TEM (HAADF-STEM) and STEM energy dispersive X-ray spectroscopy (STEM-EDS) maps were collected on an FEI Talos F200X S/TEM at an accelerating voltage of 200 kV. Powder X-ray diffraction (XRD) data were collected on a Bruker D-8 Advance X-ray Diffractometer using Cu Kα radiation.

Discussion

In order to expand the library of possible multicomponent nanoparticles, as well as understand which factors affect the selectivity of deposited materials, we set out to combine the existing partial cation exchange methods[13,40,52] with seeded growth techniques in order to produce

novel systems not possible with either techniques alone. Copper sulfide nanorods, made using a procedure from Fenton et. al.,[13] were chosen due to the ability to produce segmentation through the exchange process that would result in asymmetric Pt deposition. In a typical Cd^{2+} exchange reaction on these $Cu_{2-x}S$ rods, 245mg of cadmium (II) acetate dihydrate, 2mL of octadecene, 15mL of benzyl ether and 8mL of high purity oleylamine were combined in a 3-neck flask and heated to 100°C for 60 minutes, after which the reaction was placed under argon and cooled to 50°C. 12mg of the $Cu_{2-x}S$ nanorods were resuspended in 3mL of trioctylphosphine and sonicated for 45 minutes.

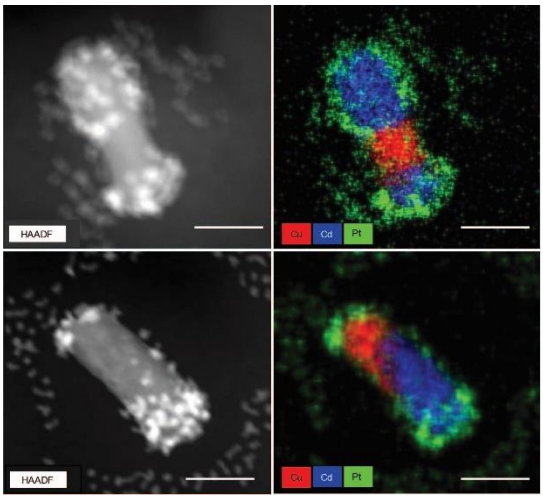

Figure 4 Pt deposition on $Cu_{2-x}S$-CdS nanorods. (A) HAADF STEM image and (B) EDS map of Pt deposition on CdS-$Cu_{2-x}S$-CdS rod. (C) HAADF STEM image and (D) EDS map of Pt deposition on $Cu_{2-x}S$-CdS rod. Scale bars are 20 nm.

These particles were then injected into the cadmium solution and allowed to react at 50° C for 60 minutes. The reaction was then quenched by injection of 8 mL of ice-cold acetone into the flask, and the flask was placed into an ice bath before being washed with IPA and hexanes three times. In contrast, in a Cd^{2+} exchange on $Cu_{s-x}S$ spheres made using a procedure from Fenton et. al.[13], 15 mg of the spheres are suspended in 3 mL of trioctylphosphine and the Cd solution is cooled to room temperature before the spheres are injected and then this reaction is allowed to run for 210 minutes to achieve roughly 50% exchanged $Cu_{2-x}S$-CdS spheres. This difference in conditions is due to the higher reactivity of the $Cu_{2-x}S$ spheres as compared to the rods or plates observed by Fenton et. al.[13] These rods and spheres were then used in the same Pt deposition reaction from Fenton et. al.[13], in which, approximately .75 mg of $Cu_{2-x}S$ spheres or rods would be dispersed in .5mL of ODE and then added to 5 mg of Pt(acac)2, 7 mL of ODE, and 50 µL of tg-OLAM in a three-neck flask. This reaction was heated under vacuum to 50°C for 30 minutes, following which the reaction was placed under blanket of Ar after 3 cycles with vacuum and Ar. The reaction temperature was raised to

130°C and allowed to react at this temperature for 150 minutes before being cooled to room temperature and washed with IPA and hexanes three times.

The platinum deposition was observed on the copper sulfide-cadmium sulfide rods using HAADF STEM and EDS STEM in order to determine where the platinum domains grew with respect to the two materials. Due to the similarity in contrast, in TEM images, between $Cu_{2-x}S$ and CdS, an EDS map that shows the location of each of the elements is required to properly differentiate the two domains.[54] The contrast in HAADF images is approximately proportional to the atomic number of the elements in the material squared.[55] In the case of $Cu_{2-x}S$ and CdS, the similarity is due to the fact that there is slightly less than double the number of copper ions as cadmium ions in these materials, which brings the effective contrast of these two in line with each other. This makes it difficult to determine which domain is comprised of which material, even if a distinction between the two can be seen. Though, sufficiently large contrast differences, such as between platinum and the two sulfides, makes identification of platinum domains significantly easier via HAADF STEM.

Surprisingly, EDS mapping showed that the rods exhibited material selectivity that was generally opposite of what the previously studied spherical nanoparticles of the same composition had. Figure 5 panel B shows nanorods with platinum deposition on both tips, but only on the length of the cadmium sulfide domain, never on the length of the copper sulfide. The experiment was repeated using partially exchanged rods with two cadmium sulfide domains to investigate whether the higher energy of tips was responsible for the deposition on the copper sulfide. This was confirmed via EDS mapping with the rods showing platinum decorating the entire cadmium sulfide domain, with the copper sulfide side remained mostly uncovered. Thus, while the increased surface area and likely imperfect ligand passivation of the tips promoted deposition[48], the observed material-based selectivity was completely opposite of what had been observed in the smaller spherical copper sulfide/cadmium sulfide particles. In order to determine the reason for

the change in selectivity of the platinum deposition on partially exchanged copper sulfide-cadmium sulfide nanorods as compared to the previously studied spheres, we investigated how selectivity could be tuned from one material to another by studying the effects of different reaction conditions on the selectivity.

Factors affecting Deposition on Nanorods

One potential explanation for the change in deposition selectivity we observed, was that the reaction conditions were based on the mass of $Cu_{2-x}S$-CdS particles, not the total surface area of the particles, which could have led to an excessive concentration of the platinum precursor, platinum (II) acetylacetonate or the reducing agent, oleylamine. If either of these compounds were too concentrated, the rate of reduction of the platinum during the nucleation phase of the reaction could have driven the reaction toward a kinetic product rather than the thermodynamic product. In this case, nucleation on the CdS domain may have been favored due to its observed ability to support nucleation at multiple sites causing the subsequent growth to favor the CdS simply because there were more Pt nucleation events on the CdS. We expected that decreasing the rate at which the platinum was reduced would limit the nucleation to the most thermodynamically preferred sites since the nucleation in other locations would be less likely to overcome the energy barrier to forming a sufficiently large nucleus

Starting with conditions identical to those used in the standard synthesis of $Cu_{2-x}S$-CdS-Pt rods, the concentration of oleylamine, platinum (I acetylacetonate and the seed nanoparticles were increased by a factor of four. This essentially scaled up the reaction without increasing the volume of solvent used and was done both as a test of the effect this would have on the deposition as well as to help ensure a sufficient amount product was recovered with each reaction. Since this

did not affect the deposition growth pattern, we used these higher concentrations in our further investigations.

Experimentally, reducing the concentration of oleylamine by half, from 100 μL to 50 μL, led to a decrease in the number of platinum domains on the rods, though their size remained consistent (~3-5 nm). Similarly, using 150 μL and 200 μL of oleylamine simply resulted in the

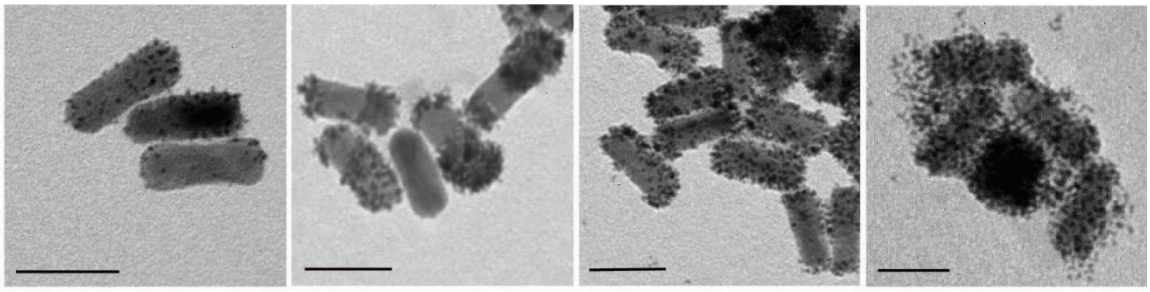

Figure 5: Pt deposition on $Cu_{2-x}S$-CdS nanorods using different OLAM concentrations. Scale bars are 50 nm.

formation of more platinum domains of this same size. The rods appeared to maintain selectivity for the CdS domains at 150 μL of oleylamine, while the particles were completely covered by Pt domains in the 200 μL sample. Even when using 50 μL of the Pt seemed to nucleation on the CdS domains. The CdS could be identified due to the slight etching of the $Cu_{2-x}S$ domains that occurred on this sample of partially nanorods due to the presence of TOP.[56] The only change in selectivity observed was with 200 μL of oleylamine where Pt domains covered both the $Cu_{2-x}S$ and the CdS segments completely. This was due to the faster reduction rate of Pt leading to a more indiscriminate burst of nucleation rather than a controlled nucleation and subsequent growth. The lack of a reversal in selectivity indicated that the reducing agent concentration can tune the degree of selectivity but not which material the Pt is selective for.

As can be seen in Figure 5 and Figure 6, platinum particles surround the nanorods in both samples. These free platinum particles indicate that the reaction conditions are not optimal for the seed mediated deposition, with a significant amount of the platinum being wasted in an undesired side reaction. Due to their smaller size, these free platinum particles can be removed during the

selective precipitation of the larger $Cu_{2-x}S$-CdS-Pt particles, but the competing reaction can limit the range of conditions that can be probed if those conditions favor the homonucleation reaction too heavily. Having a preexisting active site upon which to nucleate should lower the energy barrier for this process and thus favor growth on, in this case, the surface of the nanorod. In order to determine whether the homonucleated Pt was the more favorable product or the standard reaction conditions simply used too much platinum (II) acetylacetonate, we ran a series of experiment varying the concentration of the platinum precursor.

Due to the washing process, the amount of homonucleation is difficult to quantify, but at low concentration of oleylamine, fewer Pt domains were present on the rods, while the first wash always left a dark, opaque supernatant. This indicated that, at lower concentrations of platinum (II) acetylacetonate, most of the platinum that was reduced formed small, free particles that did not precipitate well in a hexane/ethanol solvent/antisolvent mix. As the concentration of the platinum precursor was increased from 10 mg to 15 and then 20 mg, the amount of heteronucleated Pt increased noticeably. At these higher concentrations, the Pt domain did retain some selectivity toward the CdS, with rods exhibiting less growth on the middle segments than the tips, though, as with higher concentrations of oleylamine, indiscriminate nucleation became more common. Since, the reduction was still able to overcome the activation energy for homonucleation, this process appeared to be preferred thermodynamically over the nucleation on either $Cu_{2-x}S$ or CdS surfaces.

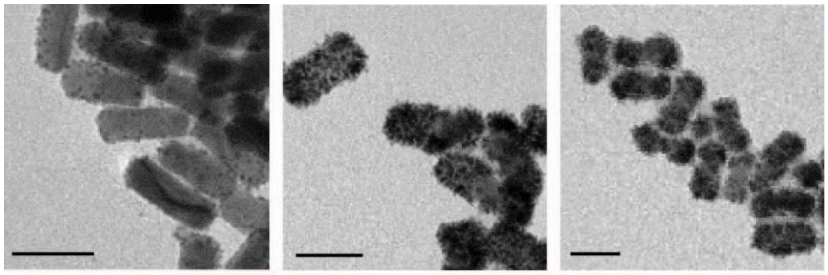

Figure 6: Pt deposition on Cu2-xS-CdS nanorods using different amounts of $Pt(acac)_2$. Scale bars are 50 nm.

Interestingly, a larger amount of platinum (II) acetylacetonate did not result in larger Pt domain sizes as would be expected if more reduction occurred the growth stage. Instead, as can

be seen in Figure 7, the rods exhibited more platinum domains of approximately the same size. Typically, in the case of "dumbbell" particles, once a nucleus has formed, further reduction will prefer growth on that domain over new nucleation events in order to minimize the less favorable interface between the seed material and depositing material. If the free surface energy of the systems could be lowered by forming a larger interface between the two materials, the particle would adopt a core-shell morphology, due this the more favorable interface.[57] In this case, however, it is likely that, in its role as a ligand, oleylamine stabilized the Pt domains at ~3-5nm. This is similar to what is observed in the synthesis of Pt seeds developed by the Sun group that uses oleylamine and oleic acid. This could also explain the unusual morphology of the Pt domains observed on the partially exchanged spheres[13] if the oleylamine was able to stabilize the domains at smaller radii than the domain eventually grew to. Rather than form the more stable, lower surface area spherical morphology, the Pt was able to maintain a "fuzzy" or "spikey" morphology. Ultimately, since neither the ratio of platinum nor oleylamine to the surface sites on the nanorod reversed the observed selectivity, we concluded that, at the very least, the change in selectivity was due to another difference between the partially exchanged rods and spheres.

Since the selectivity observed on the partially exchanged rods was inverse of what was found on the spheres and the concentration of reducing agent and platinum precursor did not alter the type of selectivity observed, it stands to reason that there must be more than the rate of reduction at play. In an attempt to understand this reversal, we sought to explore the process of deposition over time. Conditions were chosen to match the reaction with partially exchanged spheres, albeit with a lower concentration of platinum precursor (75%) and oleylamine (50%), in order to avoid excessive nucleation. Early aliquots, surprisingly, showed selectivity that matched that of the spheres, with platinum depositing on the copper sulfide domains. This deposition was not evident via brightfield TEM or HAADF STEM, however, EDS showed platinum signal colocalized with the signal for copper. Since HAADF STEM did not show any brighter regions

that would indicate platinum domains, the signal observed through EDS must have come from thin patches or layers of platinum rather than fully formed domains. Additionally, the EDS spectrum showed that the signal for platinum was very low in the 30 minute aliquot for the copper sulfide region of the rods and barely above baseline in the 15 minute aliquot for a region containing several rods. Thus, while platinum was present in both these samples, the signal in the EDS map overexaggerated the amount of platinum, likely due to a combination of data smoothing and a shorter scan time. The appearance of platinum signal without any corresponding visible domains in the HAADF STEM image, as well as the low platinum signal that was relatively uniform over the copper sulfide segment, implied that the platinum formed a thin shell on the copper sulfide domain during the first 30 minutes.

After 60 minutes, discreet domains of platinum began to appear primarily on the cadmium sulfide domain. The domains on cadmium sulfide grew slightly and became more numerous over the course of the final 90 minutes, while the signal on the copper sulfide remained unchanged. Typically, the initial selectivity is identical to the final selectivity since the first domains to nucleate will direct the growth of that domain instead of the nucleation of new domains. A change in selectivity suggests that there is more at play in this reaction than a simple seeded growth mechanism. Since the copper sulfide domains all showed signs of etching, even in the 15 minute aliquot, the initial deposition may be due to a redox reaction with the copper sulfide. Figure 8 shows a rod in which the $Cu_{2-x}S$ segment was completely etched away leaving a platinum domain behind that occupied the same place the $Cu_{2-x}S$ had. This demonstrates that the etching could not have occurred prior to

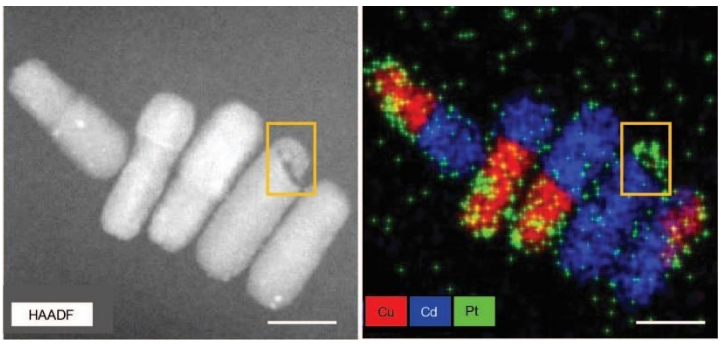

Figure 7: EDS and HAADF showing complete removal of a $Cu_{2-x}S$ domain and the platinum shell that remained after 90 minutes of reaction. Scale bars are 20nm.

the platinum deposition reaction as the would not have formed this thin cap-like structure without a $Cu_{2-x}S$ template. The HAADF STEM image also showed etching of the $Cu_{2-x}S$ at the interface of the two sulfide domains suggesting that this interface promoted the etching process, possibly due to interfacial strain.[58]

The etching could be caused by a redox reaction in which either copper(I) or the S^{2-} are oxidized, in a manner similar to observations by Manna[59] with PbSe and CdTe and Banin[60] in the case of CdS. This would explain the limited nature of the initial deposition, as the shell that forms could inhibit further reaction unless the interface between the CdS and $Cu_{2-x}S$ allowed the reaction to bypass this shell, leading to the oleylamine becoming the dominant reducing agent. If the CdS surface was then the preferred surface for nucleation due to surface defects, for example, this could explain the nucleation and subsequent growth of Pt domains on the CdS while the shell on the $Cu_{2-x}S$ did not change after the 30 minute timepoint. Neither the copper(I) nor the sulfide oxidation mechanism alone, however, can account for the differences between the spheres and rods, as these mechanisms should be consistent across the two systems. If, however, the surface of the CdS was not as active, due to less surface defects for example, then the initial deposition of Pt on the $Cu_{2-x}S$ might have dictated the subsequent growth on that domain. A more careful investigation of the deposition process on the spheres was required to understand the selectivity inversion the difference in deposition between these two systems.

Mixed population of CuS and CdS spheres

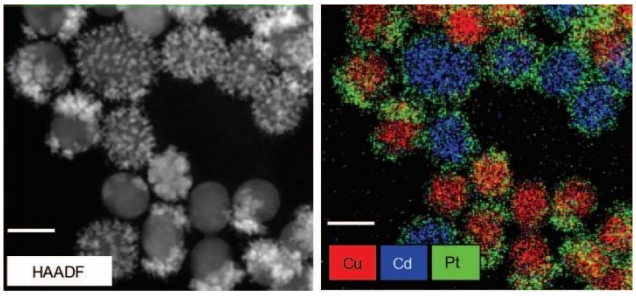

Figure 8: Platinum growth patterns observed on mixed population of $Cu_{2-x}S$ and CdS spheres. Scale bars are 30 nm.

In an effort to compare the deposition of platinum on the rod-like particles to the spherical particles, with the least number of convoluting factors possible, we chose to study the growth of platinum on a mixed population of $Cu_{2-x}S$ and fully exchanged CdS spheres. In order to prepare the fully exchanged rods with the fewest synthetic modifications, we chose to use the same reaction conditions, specifically 50° C for 60 minutes, rather than the room temperature for 210 minutes conditions designed to achieve partially exchanged spheres. The choice to switch to a mixed population spherical particles, each containing a single material domain, was aimed at simplifying the system as much as possible while still being able to observe the competition between the nucleation and growth on the two materials. In particular, this eliminated the interface, which we have already seen have an affect the deposition reaction.

Interestingly, under the same conditions used for the previous nanorod reactions, there was no obvious selectivity, but there was a stark difference in growth pattern. The platinum on copper sulfide formed single, “fuzzy” domains while, on the cadmium sulfide, it produced a patchy pattern of many distinct, smaller domains. This pattern seems to be in line with the hypothesis that the growth on the CdS may be due to surface defects that arise from the exchange

reaction. Alivisatos has shown that cation exchange reactions can result in nanoparticles with a much higher number of defects if the kinetics of exchange are faster than the defects can anneal out.[61]

In this case, the larger, coalesced platinum domains on the $Cu_{2-x}S$ spheres, which matched the deposition observed on the partially exchanged spheres[13], might have been due to $Cu_{2-x}S$ being the preferred material, but differences in the cation exchange step might have led to the formation of surface defects on the CdS that resulted in a competing nucleation process. In order to explore this possibility, we studied the effects of oleylamine concentration, in addition to an aliquot study, as a comparison to data previously gathered for the partially exchanged rods. Additionally, we investigated the effects of temperature on the selectivity and growth pattern of platinum on the mixed population of spheres.

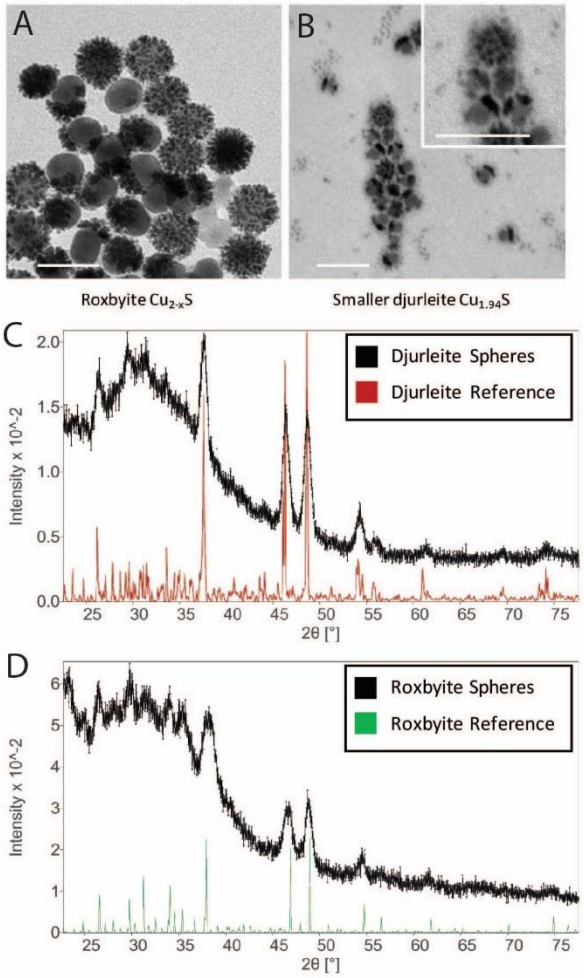

Figure 9: (A) TEM of deposition of Pt on $Cu_{2-x}S$ and (C) XRD of $Cu_{2-x}S$ made using roxbyite procedure from Fenton et. al.[13] (B) TEM Pt deposition on $Cu_{1.94}S$ and CdS spheres and XRD of $Cu_{1.94}S$ made using djurleite procedure from Robinson et. al.[52] Scale bars are 50 nm.

Attempts to study the deposition of platinum over time through an aliquot study did show some initial deposition of platinum on the $Cu_{2-x}S$ spheres. However, issues with precipitation of the CdS-Pt particles prevented an analysis of the full sample. An explanation of the problem encountered with CdS-Pt particle and how to mitigate it can be found below. Without data on how the reaction proceeds on the CdS-Pt, it is difficult to draw conclusions, but the data we do

have seems in line with what we observed with the partially exchanged rods, with growth of a thin shell of Pt first on $Cu_{2-x}S$ and then eventually nucleation on the CdS. The lack of platinum signal colocalized with the Cd signal indicates that the Pt growth is only on the $Cu_{2-x}S$ spheres during the initial stages of the reaction. Interestingly the Pt shell seems to appear very early in the reaction at 5 minutes. This is likely the case with both rods and spheres, however, during our aliquot study on the rods, we took our first aliquot at 15 minutes, so we cannot be certain that the shell forms this early in both samples. Since these conditions are the same as the ones used in the previous samples, the CdS-Pt should match our previous observations at the final 150-minute time point. Under this assumption, the growth processes would appear to be the same on both the mixed population spheres and the partially exchanged rods. Unfortunately, due to reproducibility issues with the $Cu_{2-x}S$ spheres, a new procedure from the Macdonald group[52] had to be used for subsequent experiments. This reaction produced smaller djurleite $Cu_{1.94}S$ spheres, but the same cation exchange procedure was used on these spheres and they exhibited the same growth patterns as previously observed.

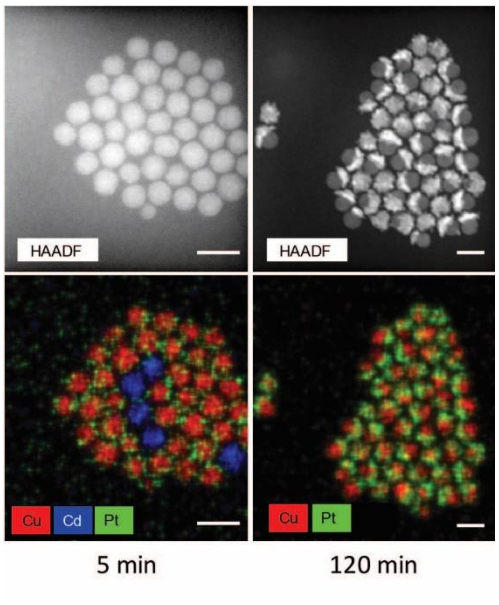

Figure 10: HAADF STEM and EDS maps 5 min and 120 min aliquot of Pt growth on mixed CdS and $C_{2-x}S$ spheres. Scale bars are 20 nm.

To test the effects of temperature during deposition, we performed the platinum deposition reaction under the same conditions at several different temperatures. It was expected that higher temperatures would lead to more numerous, but less selective nucleation than lower temperatures simply because the increase in energy would enable nucleation at active sites that were less active on the surface of both materials. This was not predicted to significantly effect deposition on the CdS spheres as they already showed a large number of Pt domains, again

possibly due to surface defects from the exchange process. Conversely, at lower temperatures, we expected fewer domains, since there might not be enough energy to form stable nuclei at as many sites and the lower temperature would diminish the reducing power of the oleylamine, which would lead to less Pt deposition overall. This lessening in reducing power might also lead to a shift toward less nucleation and more growth as the Pt reduces more slowly. Experimentally, lowering the temperature to 100° C drastically decreased the amount of platinum on both cadmium sulfide and copper sulfide spheres. Unfortunately, due to the fact that the homonucleated platinum precipitates very poorly, it is difficult to accurately gauge the relative amount of platinum that reduced this way. However, the presence of some free platinum, indicates that the homonucleation persists at temperatures lower than the heteronucleation under these conditions, which makes exploring these temperatures difficult. Increasing the temperature to 160° C resulted in platinum on both spheres, similar to what was seen at 130° C, but with a portion of the copper sulfide particles showing multiple platinum domains, as expected for a more indiscriminate nucleation. Additionally, at 160° C, the CdS spheres exhibited larger Pt domains, indicating either a shift toward the growth stage or possibly an Ostwald ripening process[62], in which the smaller, less stable Pt domains on CdS dissolve to the more stable domains grow.

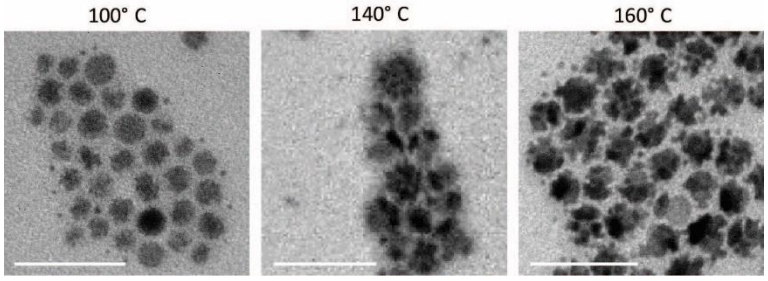

Figure 11: Pt deposition on $Cu_{1.94}S$ and CdS spheres at different temperatures. Scale bars are 50 nm.

These results demonstrated that, without a way to mitigate the homonucleation, it may not be possible to fully exploit the differences between these two materials under these reaction conditions. It may be possible to suppress the homonucleation by using a binding ligand that binds more weakly to the Pt, such as a carboxylic acid, and of course a different reducing agent,

to make it more energetically unfavorable to form the initial platinum nuclei. A weaker ligand should stabilize the early nuclei less, thereby promoting the heteronucleation of the Pt. This, however, was deemed to be beyond the scope of the investigation and, accepting that homonucleation was unavoidable, a slightly higher temperature, 140^{o} C, was used for all of the following reactions to ensure sufficient nucleation for comparison of the differences in nucleation and growth.

Following the same logic as in the experiments with the partially exchanged rods, it was expected that lower concentrations of the reducing agent, oleylamine, would lead to less overall Pt deposition, potentially with more selectivity toward the most active material, while higher concentrations would lead to more indiscriminate deposition. Additionally, we hoped to see an indication of what made the deposition on the rods different from the spherical particles. The CdS spheres used in these experiments had a subpopulation that were not fully exchanged, however these partially exchanged spheres were not included in the analysis of the sample because it is not always clear where Pt deposited on these particles relative to the sulfide segments in a two-dimensional projection of these spheres.

Decreasing the amount of oleylamine by 75%, from 100 to 25uL, lead to a number of copper sulfide nanoparticles without significant platinum deposition, which seemed to indicate selectivity, under these conditions, toward the CdS. This also changed the morphology of the platinum domains on the cadmium sulfide nanoparticles from the patchy pattern previously observed to a more “fuzzy” single domain, which can be attributed to a slower reduction rate on both materials shifting the reaction away from the nucleation stage and allowing for more growth of the existing domains. The change in both selectivity and growth pattern, would appear to support the idea that the surface of the CdS particles was preferred over the $Cu_{1.94}S$ due to a

number of active sites or defects that promote the nucleation of the Pt domains. The difference between these two surfaces may be very large, since, while a portion of the $Cu_{1.94}S$ showed little or no deposition, the number of Pt domains on the CdS also decreased, indicating that the most active sites on the CdS were still in competition with the surface of the $Cu_{1.94}S$.

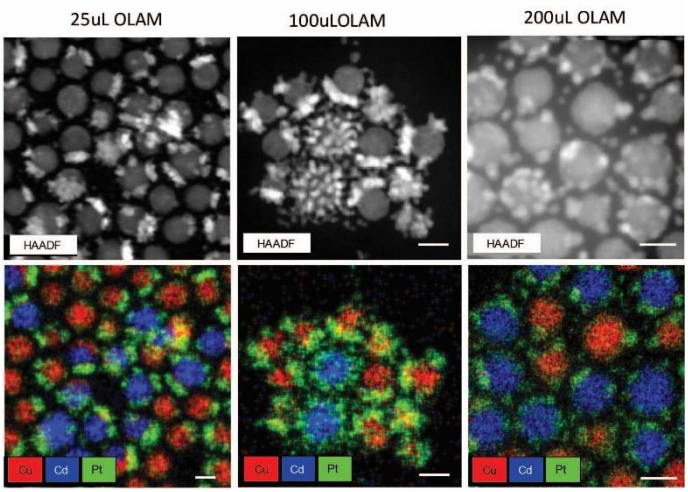

Figure 12: HAADF STEM and EDS maps of Pt deposition on $Cu_{1.94}S$ and CdS spheres at different OLAM concentrations. Scale bars are 10 nm.

Increasing the amount of oleylamine from 100 to 200 μL resulted in $Cu_{1.94}S$ particles with noticeably smaller Pt domains than either the 100 μL or the 25 μL samples. At the same time, the CdS particles exhibited fewer domains of Pt, with some particles looking very similar in the HAADF STEM image to the $Cu_{1.94}S$ spheres. The decrease in the overall amount of Pt can likely be explained by an increase in homonucleation, though this could not be verified without additional characterization of the supernatant. On the other hand, the similarity in number and size of the domains on $Cu_{1.94}S$ and CdS implied that the higher concentration of the reducing agent led to indiscriminate nucleation and growth, where the differences between materials was not enough to produce any significant selectivity difference as conditions were such that nucleation could occur at any suitable location instead of only the most active. The fact that some CdS particles did still show a large number of nucleations indicated that there were still the same number of potential sites on all of the CdS spheres, but under these conditions, only a portion of these enabled nucleation for kinetic reasons.

Role of oleylamine and trioctylphosphine as ligands

Since oleylamine functions as both reducing agent and ligand, it can be difficult to separate the role ligand environment plays in reactions like this platinum deposition reaction. In order to determine whether the ligation played a role in the selectivity reversal between partially exchanged rods and spheres, the copper sulfide and cadmium sulfide particles were sonicated in 5mL of oleylamine before being washed, re-dispersed in hexanes and used as seed particles in the platinum growth reaction. Since the cadmium exchange reaction utilizes trioctylphosphine as a soft base, which may act as a ligand on the cadmium sulfide particles, this modification was designed to eliminate any differences in the ligation of the two materials from the cation exchange reaction, as the oleylamine should replace the trioctylphosphine. The sterically bulkier trioctylphosphine, could have resulted in lower surface coverage which would have increased the surface energy of the cadmium sulfide, resulting in the relatively higher platinum deposition at lower oleylamine concentrations.

Experimentally, however, there was no clear change as compared to samples that had not been pre-sonicated in oleylamine. There was, however, a much larger amount of homonucleated Pt in these samples, likely due to an effective increase in the amount of oleylamine present in the reaction. This homonucleation made characterization difficult, particularly the determination of what was free Pt and what was an attached Pt domain, due to the two-dimensional nature of HAADF STEM and EDS mapping. While tomography could be used to help mitigate this, we determined that this line of inquiry would require a significantly larger investigation and would be more suitable for a future study. While not

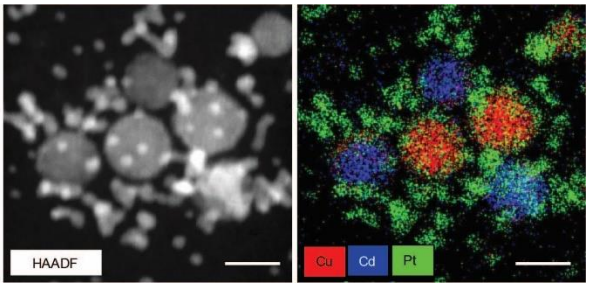

Figure 13: EDS and HAADF of samples after OLAM sonication and Pt growth

investigated further in this study, the potential for ligands to effect selectivity in multicomponent nanoparticles systems remains a promising way to direct growth of additional domains via seeded growth methods.

Evidence of surface changes

Following the platinum deposition reaction on the mixed population of spherical nanoparticles, cadmium sulfide-platinum was absent from the final washed product in most experiments. Initially this was believed to be due to dissolution of the cadmium sulfide during the reaction. However, this would have required a redox reaction with the platinum (II) acetylacetonate, which was considered unlikely given lack of reaction on the partially exchanged rods and spheres. The other alternative was that the particles were intact, but simply not precipitating during the washing. While the ligand environment of the cadmium sulfide-platinum should have been similar to the corresponding copper sulfide-platinum particles, as well as, the cadmium sulfide seed, the increased surface coverage of the platinum domains might have been sufficient to alter the dispersibility of the particles. Using a more polar antisolvent, acetone, was sufficient to precipitate the cadmium sulfide-platinum nanoparticles. These particles did not show any signs of etching or other morphology change that would suggest a redox reaction with the platinum (II) acetylacetonate.

The exact cause for this change in dispersibility was not thoroughly investigated, but it stands to reason that the increased number of Pt domains resulted in a more polar tolerant surface by altering the ligand environment in some way. Since both the $Cu_{1.94}S$-Pt particles and the CdS seed particles continued to precipitate as expected, either the more uniform coverage of the Pt domains on the CdS led to this change or the resultant curvature of the CdS-Pt surface affected the ligand packing. In this reaction, the only possible ligands were oleylamine and any

trioctylphosphine left over from the exchange reaction, though in both cases these would be present on the CdS seeds, indicating that neither of these were responsible for the change. This makes it unlikely that the difference in binding of either ligand to Pt would alter the ligand environment much, in and of itself. Thus, it is likely that the morphology of the particle disrupted the ligand packing leading to insufficient ligation.

Presence of Cu and effects of co-deposition with Pt

In a number of samples, both partially exchanged rods and mixed spheres, EDS mapping showed colocalization of Cu and Pt in newly formed Pt domains. This Cu region did not overlap with S signal that would indicate that this was a copper sulfide like $Cu_{2-x}S$. This was the case on both CdS and $Cu_{1.94}S$ spheres and both segments of the partially exchanged nanorods and coincides with decreases in selectivity and changes in growth pattern on the sphere. In particular, CdS-Pt spheres with this colocalization of copper and platinum had significantly fewer platinum domains and these domains were larger than normal. The deposition of small copper domains, thus, appeared to seed the growth of the Pt. Alternatively, copper and platinum are miscible and the colocalization could indicate an alloy core with additional platinum grown on top, though determining whether the core is an alloy or purely copper with platinum above and below is not possible with EDS alone. In either case, the presence of copper in these platinum domains seemed to alter the deposition process in these samples significantly.

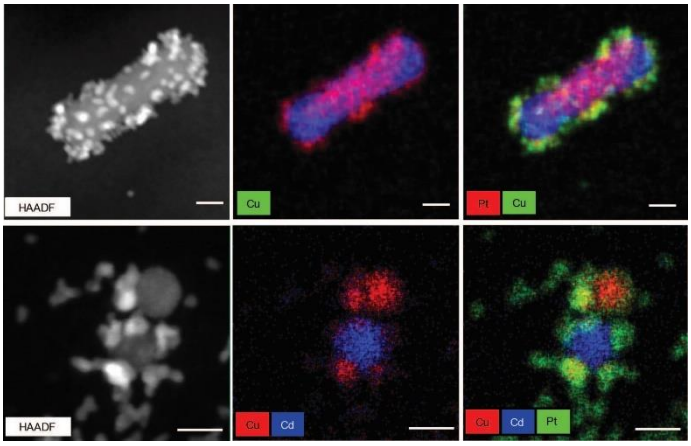

Figure 14: HAADF and EDS maps showing colocalized Pt and Cu after deposition reaction on $Cu_{2-x}S$-CdS rods and $Cu_{1.94}S$ and CdS spheres. Scale bars are 10 nm.

HAADF STEM images of the rod samples also showed evidence of etching on the $Cu_{2-x}S$ domain, which is known to occur in presence of trioctylphosphine. Unlike the etching observed in other rod samples, the presence of large copper domains on both particles seems to be acting as a seed for the growth of platinum rather than as a sacrificial material. Additionally, the presence of Cu in the core of these platinum domains seemed to indicate that the copper was present in the reaction before platinum deposition began, again in contrast to the dissolution as Pt deposited, as seen previously. This suggests that the trioctylphosphine used in the cadmium exchange reaction etched the copper sulfide and then the copper redeposited during the platinum growth reaction. Incomplete washing of the exchanged seed particles then would explain the presence of copper ions during these reactions and consequently the changes in morphology and selectivity exhibited by these samples. The use of an initial seed material to promote and control the deposition of a less selective material may be a promising method of control in systems in which the seed material is inert.

Conclusions

From our investigation into the nucleation and growth of Pt on $Cu_{2-x}S$-CdS nanorods, there are several important observations that will aid in our ability to synthesize hybrid nanoparticles through a combination of partial cation exchange and seeded growth techniques. We observed two potential methods for altering the selectivity of the Pt domains, via controlling the kinetics of reaction and via the introduction of initial seed domain like metallic Cu. The co-deposition of copper with the platinum seen in a subset of samples did appear to affect the deposition pattern on the mixed population of spheres, and while this was independent of the previous shell formation where no copper was present in the platinum, it does illustrate that changes to the initial nucleation are key to the selectivity. The observed etching of the copper

sulfide domain, coupled with the deposition of what appeared to be a thin Pt shell during the initial stages of the reaction, may be worth further investigation as it was able to completely dissolve $Cu_{2-x}S$ domains while depositing the Pt shell. Understanding this process may be useful, not only in preventing damage to partially exchanged particles, but also in enabling alternate deposition methods.

More importantly, we observed a reversal of material selectivity, with respect to the deposition of Pt, from $Cu_{2-x}S$ to CdS. From our data, we are able to hypothesize that the difference in selectivity is due to active sites on the surface of the cadmium sulfide domain that formed as a result of the cation exchange process, similar to observations made by Banin with the deposition of Au onto CdS rods.[60] The defect induced growth reported by Banin appeared to be linked to the presence of air during the deposition reaction, while our reaction was run under a blanket of argon. These defects likely come from the difference in temperature of the partial cation exchange reactions used on the spherical particles of $Cu_{1.94}S$ and the $Cu_{2-x}S$ rod-like particles.[61] Due to the rapid exchange rate of the spherical particles with Cd^{2+} the reaction was run at 25°C rather than 50°C to achieve a more consistent product. This change likely resulted in fewer surface defects, which, in turn, resulted in the platinum nucleating on the $Cu_{2-x}S$ domain since there were no defects sites to promote nucleation on the CdS. However, this hypothesis requires further investigation, as other factors, such as ligand environment may be able to explain the selectivity reversal. Testing the deposition of Pt on partially exchanged spheres made using shorter times at 50°C will be imperative in determining whether the selectivity difference is due to surface defects.

Exploring alternate cation exchange conditions may be another area worth pursuing as this may elucidate the role of surface defects. The cadmium exchange is uniquely fast compared to other similar exchanges under the same conditions, potentially leading to a higher defect density, which in turn could explain the larger number of smaller noble metal domains observed on the

partially exchanged rods, spheres and even plates, as well as the fully exchanged spheres. Additionally, it would be worth exploring other partially exchanged systems, particularly ones that lack one or both of copper sulfide and cadmium sulfide, in order to both explore the selectivity in these systems and to compare to the systems explored in this investigation. Determining whether unexpected results, such as the apparent platinum shell formation and corresponding etching of copper sulfide, are important factors in the deposition reaction will be important as these systems become more complex. Additionally, partial cation exchange conditions that lead to double capped rods, such as with zinc sulfide-copper sulfide-zinc sulfide, should be explored as these systems may enable the deposition on the sides in a controllable fashion. This is an important parameter in systems like photocatalytic nanoparticles where the distance between the active components needs to be controlled limited.[7] Similarly, exploration of deposition on systems in which a gold exchange is not possible, like zinc sulfide-cadmium sulfide, are worth exploring in order to expand the library of accessible systems. Since Au^{3+} is softer than Zn^{2+} or Cd^{2+}, an additional cation exchange reaction of copper sulfide with zinc prior to the seeded growth could have prevented any undesired cation exchange reactions.

References

1. Chen, J.; Jiang, Z.; Ackerman, J. D.; Yazdani, M.; Hou, S.; Nugen, S. R.; Rotello, V. M. Analyst 2015, 140, 4991-4996.

2. Kyriazi, M.; Giust, D.; El-Sagheer, A. H.; Lackie, P. M.; Muskens, O. L.; Brown, T.; Kanaras, A. G. ACS Nano 2018, 12, 3333−3340.

3. Xu, C.; Xie, J.; Ho, D.; Wang, C.; Kohler, N.; Walsh, E. G.; Morgan, J. R.; Chin, Y. E.; Sun, S. Angew. Chem. Int. Ed. 2008, 47, 173 –176.

4. Wu, K.; Chen, Z.; Lv, H.; Zhu, H.; Hill, C. L.; Lian, T. J. Am. Chem. Soc. 2014, 136, 7708−7716

5. Wang, C.; Yin, H.; Dai, S.; Sun, S. Chem. Mater. 2010, 22, 3277–3282.

6. Maeda, K.: Domen, K. J. Phys. Chem. Lett. 2010, 1, 2655–2661.

7. Amirav, L.; Alivisatos, A. P. J. Phys. Chem. Lett. 2010, 1, 1051–1054

8. Dukovic, G.; Merkle, M. G.; Nelson, J. H.; Hughes, S. M.; Alivisatos, A. P. Adv. Mater. 2008, 20, 4306–4311

9. Kim, C. S.; Mout, R.; Zhao, Y.; Yeh, Y.-C.; Tang, R.; Jeong, Y.; Duncan, B.; Hardy, J. A.; Rotello, V. M. Bioconjugate Chem. 2015, 26, 950−954.

10. Hodges, J. M.; Biacchi, A. J.; Schaak, R. E. ACS Nano 2014, 8, 1047-1055.

11. Hodges, J. M.; Schaak, R. E. Acc. Chem. Res. 2017, 50, 1433-1440.

12. Crane, C. C.; Tao, J.; Wang, F.; Zhu, Y.; Chen, J. J. Phys. Chem. C 2014, 118, 28134−28142.

13. Fenton, J.L.; Steimle, B.C.; Schaak, R.E. Science 2018, 360, 513-517.

14. Smith, W. C.; Morse, J. R.; Bria, C. R. M.; Schaak, R. E.; Williams, S. K. R. ACS Appl. Nano Mater. 2018, 1, 6435−6443.

15. Menagen, G.; Mocatta, D.; Salant, A.; Popov, I.; Dorfs, D.; Banin, U. Chem. Mater. 2008, 20, 6900–6902.

16. Naskar, S.; Schlosser, A.; Miethe, J. F.; Steinbach, F.; Feldhoff, A.; Bigall, N. C. Chem. Mater. 2015, 27, 3159−3166

17. J.M. Hodges, J.L. Fenton, J.L. Gray, R.E. Schaak, Nanoscale 2015, 7, 16671-16676.

18. Thanh, N. T. K.; Maclean, N.; Mahiddine, S. Chem. Rev. 2014, 114, 7610−7630.

19. Trentler, T. J.; Hickman, K. M.; Goel, S. C.; Viano, A. M.; Gibbons, P. C.; Buhro, W. E. Science 1995 270, 5243, 1791-1794.

20. Motl, Ne. E.; Bondi, J. F.; Schaak, R. E. Chem. Mater. 2012, 24, 1552-1554.

21. Gordon, T. E.; Schaak, R. E. Chem. Mater. 2014, 26, 5900-5904.

22. Read, C. G.; Gordon, T. R.; Hodges, J. M.; Schaak, R. E. J. Am. Chem. Soc. 2015, 137, 12517-12517.

23. Jiang, Y.; Huo, S.; Mizuhara, T.; Das, R.; Lee, Y.-W.; Hou, S.; Moyano, D. F.; Duncan, B.; Liang, X.-J.; Rotello V. M. ACS Nano 2015, 9, 9986–9993.

24. Wang, C.; Yin, H.; Dai, S.; Sun, S. Chem. Mater. 2010, 22, 3277–3282 3277

25. Brust, M.; Walker, M.; Bethell, D.; Schiffrin, D. J.; Whyman, R. J. Chem. Soc., Chem. Commun. 1994, 801-802.

26. Cirri, A.; Silakov, A.; Jensen, L.; Lear, B. J. J. Am. Chem. Soc. 2016, 138, 15987−15993

27. Biacchi, A. J.; Schaak, R. E. ACS Nano 2015, 9, 1707-1720.

28. Cao-Milán, R.; He, L. D.; Shorkey, S.; Tonga, G. Y.; Wang, L.; Zhang, X.; Uddin, I.; Das, R.; Sulakc, M.; Rotello, V. M. Mol. Syst. Des. Eng., 2017, 2, 624

29. Hostetler, M. J.; Templeton, A. C.; Murray, R. W. Langmuir 1999, 15, 3782-37

30. Dong, A.; Ye, X.; Chen, J.; Kang, Y.; Gordon, T.; Kikkawa, J. M.; Murray, C. B.

31. Buck, M. R.; Bondi, J. F.; Schaak, R. E. Nature Chemistry 2012, 4, 37-44

32. Figuerola A.; Franchini I. R.; Fiore, A.; Mastria, R.; Falqui A.; Bertoni, G.; Bals S.; Tendeloo G. V.; Kudera, S.; Cingolani, R.; Manna, L. Adv. Mater.2009,21,550–554

33. Li, P.; Wei, Z.; Wu, T.; Peng, Q.; Li, Y. J. Am. Chem. Soc. 2011, 133, 5660–5663

34. Lee, K. S.; Anisur, R. M.; Kim, K. W.; Kim, W. S.; Park, T.; Kang, E. J.; Lee, I. S. Chem. Mater. 2012, 24, 682−687

35. Maeda, K.; Domen, K. J. Phys. Chem. Lett. 2010, 1, 2655–2661

36. Bradley, M. J.; Read, C. G.; Schaak, R. E. J. Phys. Chem. C 2015, 119, 8952−8959.

37. Hodges, J. M.; Morse, J. R.; Williams, M. E.; Schaak, R. E. J. Am. Chem. Soc. 2015, 137, 15493-15500.

38. Menagen, G.; Mocatta, D.; Salant, A.; Popov, I.; Dorfs, D.; Uri Banin, U. Chem. Mater. 2008, 20, 6900–6902

39. Fenton, J.L.; Hodges, J.M.; Schaak, R.E. Chem. Mater. 2017, 29, 6168-6177.

40. Son, D. H.; Hughes, S. M.; Yin, Y.; A. Paul Alivisatos, A. P.; Science. 2004, 306, 5698, 1009-1012.

41. Li, H.; Zanella, M.; Genovese, A.; Povia,M.; Falqui,A.; Giannini, C.; Manna, L. Nano Lett. 2011, 11, 4964–4970

42. Fenton, J. L.; Schaak, R. E. Angew. Chem. Int. Ed. 2017, 56, 6464–6467.

43. Pearson, R. G. J. Am. Chem. Soc. 1985, 107, 6801-6806.

44. Parr, R. G.; Pearson, R. G. J. Am. Chem. Soc. 1983, 105, 7512-7516.

45. Groeneveld, E.; Witteman, L.; Lefferts, M.; Ke, X.; Bals, S.; Tendeloo, G. V.; Donega, C. M.; ACS Nano2013797913-7930

46. Zherebetskyy, D.; Zhang, Y.; Salmeron, M.; Wang, L.-W. J. Phys. Chem. Lett. 2015, 6, 4711−4716.

47. Fenton, J.L.; Steimle, B.C.; Schaak, R.E. J. Am. Chem. Soc. 2018, 140, 6771-6775.

48. Mokari, T.; Rothenberg, E.; Popov, I.; Costi, R.; Banin, U. Science 2004, 304, 1787–1790.

49. Lesnyak, V.; Brescia, R.; Messina, G. C.; Manna, L. J. Am. Chem. Soc. 2015, 137, 29, 9315-9323

50. Wolf, A.; Hinrichs, D.; Sann, J.; Miethe, J. F.; Bigall, N. C.; Dorfs, D. J. Phys. Chem. C 2016, 120, 21925−21931

51. Hernández-Pagán, E. A.; O'Hara, A.; Arrowood, S. L.; McBride J. R.; Rhodes, J. M., Pantelides, S. T.; Macdonald, J. E. Chemistry of Materials. 2018, 30(24), 8843-8851.

52. Robinson, E. H.; Turo, M. J.; Macdonald, J. E.; Chem. Mater. 2017, 29, 9, 3854-3857

53. Ha, D.-H.; Caldwell, A. H.; Ward, M. J.; Honrao, S.; Mathew, K.; Hovden, R.; Koker, M. K. A.; Muller, D. A.; Hennig, R. G.; Robinson, R. D. Nano Lett. 2014, 14, 7090−7099

54. Jesson, D. E.; Pennycook, S. J. Proc. R. Soc. Lond. A 1995 449, 273-293.

55. Midgley, P. A.; Weyland, M. Ultramicroscopy 2003, 96, 413–431.

56. Nelson, A.; Ha, D.-H; Robinson R. D. Chem. Mater. 2016, 28, 8530−8541

57. Han, S.; Liu, W.; Cai, C.; Cao, P; Gu, M. Part. Part. Syst. Charact, 2019, 36, 1800426

58. Kwon, S. G.; Krylova, G.; Phillips, P. J.; Klie, R. F.; Chattopadhyay, S.; Shibata, T.; Bunel, E. E.; Liu, Y.; Prakapenka, V. B.; Lee, B.; Shevchenko, E. V. Nature Materials. 2015, 14, 215–223

59. Carbone, L.; Kudera, S.; Giannini, C.; Ciccarell, G.; Cingolani, R.; Cozzoli, P. D.; Manna, L. J. Mater. Chem., 2006, 16, 3952–3956

60. Aaron E. Saunders, A. E.; Popov, I.; Banin, U. J. Phys. Chem. B 2006, 110, 25421-25429

61. Jain, P. K.; Beberwyck, B. J.; Fong, L.-K.; Polking, M. J.; Alivisatos, A. P. Angew. Chem. Int. Ed.2012,51, 2387 –2390

62. Kahlweit, M. (1975). Adv. Colloid Interface Sci. 5 (1): 1–35.